

Combining scEEG and PPG for reliable sleep staging using lightweight wearables

Jiawei Wang, Liang Xu, Shuntian Zheng, Yu Guan, Kaichen Wang, Ziqing Zhang, Chen Chen, Laurence T. Yang, *Fellow, IEEE*, Sai Gu

Abstract—Reliable sleep staging remains challenging for lightweight wearable devices such as single-channel electroencephalography (scEEG) or photoplethysmography (PPG). scEEG offers direct measurement of cortical activity and serves as the foundation for sleep staging, yet exhibits limited performance on light sleep stages. PPG provides a low-cost complement that captures autonomic signatures effective for detecting light sleep. However, prior PPG-based methods rely on full night recordings (8 - 10 hours) as input context, which is less practical to provide timely feedback for sleep intervention. In this work, we investigate scEEG-PPG fusion for 4-class sleep staging under short-window (30 s - 30 min) constraints. First, we evaluate the temporal context required for each modality, to better understand the relationship of sleep staging performance with respect to monitoring window. Second, we investigate three fusion strategies: score-level fusion, cross-attention fusion enabling feature-level interactions, and Mamba-enhanced fusion incorporating temporal context modeling. Third, we train and evaluate on the Multi-Ethnic Study of Atherosclerosis (MESA) dataset and perform cross-dataset validation on the Cleveland Family Study (CFS) and the Apnea, Bariatric surgery, and CPAP (ABC) datasets. The Mamba-enhanced fusion achieves the best performance on MESA (Cohen's Kappa $\kappa = 0.798$, Acc = 86.9%), with particularly notable improvement in light sleep classification (F1-score: 85.63% vs. 77.76%, recall: 82.85% vs. 69.95% for scEEG alone), and generalizes well to CFS and ABC datasets with different populations. These findings suggest that scEEG-PPG fusion is a promising approach for lightweight wearable based sleep monitoring, offering a pathway toward more accessible sleep health assessment. Source code of this project can be found at: <https://github.com/DavyWJW/scEEG-PPG-Fusion>

Index Terms—Sleep stage classification, wearable computing, AI for healthcare, multimodal fusion

Jiawei Wang, Liang Xu, Sai Gu are with the School of Engineering, The University of Warwick, Coventry, UK (e-mail: Davy.Wang@warwick.ac.uk; Liang.Xu.1@warwick.ac.uk; Sai.Gu@warwick.ac.uk).

Shuntian Zheng and Yu Guan are with the Department of Computer Science, The University of Warwick, Coventry, UK (e-mail: Shuntian.Zheng@warwick.ac.uk; Yu.Guan@warwick.ac.uk).

Kaichen Wang, Ziqing Zhang are with the College of Biomedical Engineering, Fudan University, Shanghai, China (e-mail: 23110720140@m.fudan.edu.cn; 25212030032@m.fudan.edu.cn).

Chen Chen is with the Human Phenome Institute, Fudan University, Shanghai, China (e-mail: chenchen.fd@fudan.edu.cn)

Laurence T. Yang is with the School of Computer and Artificial Intelligence, Zhengzhou University, Zhengzhou, China (e-mail: ltyang@gmail.com)

I. INTRODUCTION

Sleep plays a vital role in maintaining human health, affecting cognitive performance, metabolic balance, and cardiovascular regulation [1], [2]. Accurate sleep staging, as defined by the American Academy of Sleep Medicine (AASM) [3], involves classifying nocturnal recordings into wakefulness (Wake), rapid eye movement (REM), and non-REM stages (N1/N2/N3), and is essential for diagnosing sleep disorders and assessing overall sleep quality [4]. Polysomnography (PSG), the clinical gold standard, relies primarily on multi-channel electroencephalography (EEG), electrooculography (EOG), electromyography (EMG), and electrocardiogram (ECG), etc. [5], [6]. As shown in Fig. 1(a), despite its reliability, the high cost, cumbersome setup, and dependence on professional scoring restrict the scalability of PSG for daily or home-based monitoring [7]–[10]. For practical applications, a four-stage classification comprising Wake, REM, light sleep (N1+N2), and deep sleep (N3) is commonly adopted [11].

With advances in wearable sensing, wearable EEG devices have emerged as an accessible alternative for portable sleep monitoring. Fig. 1(b–e) shows representative wearable devices: (b) multi-signal systems integrating EEG, EOG, and EMG, (c) multi-channel EEG systems, (d) forehead single-channel EEG (scEEG) devices and (e) headset scEEG devices. Compared to PSG, these wearable devices offer improved portability and ease of deployment [12]. Among them, scEEG represents the most lightweight solution for home-based sleep monitoring, requiring only minimal electrode setup with significantly lower cost and improved user comfort compared to multi-signal and multi-channel systems [13], [14]. However, scEEG generally exhibits lower accuracy for detecting light sleep stage [15]–[17].

This difficulty in light sleep classification reflects challenges acknowledged by AASM guidelines, which characterize light sleep (particularly stage N1) as a transitional state with subtle EEG features that can be easily confused with Wake or REM sleep [23]. For scEEG, the limited spatial information further exacerbates this challenge, as characteristic features may not be adequately captured from a single recording site.

Research has demonstrated that different sleep stages are associated with distinct autonomic patterns, with the transition from Wake to light sleep showing pronounced shifts from sympathetic to parasympathetic dominance [24]–[26]. This suggests that autonomic signals may complement EEG par-



Fig. 1: Wearable sleep monitoring devices and the motivation for scEEG-PPG fusion: (a) clinical gold-standard PSG [7], (b) multi-signal system integrating EEG, EOG, and EMG (Tosoo AG) [13], (c) multi-channel EEG system (Greentek GT Cap) [18], (d) forehead scEEG device (Neurovista Sleep Monitor) [19], (e) headset scEEG device (Brainlink Lite) [20], (f) PPG-based smart ring (RingConn) [21], (g) PPG-based smart watch (Garmin) [22].

ticularly for light sleep identification. Photoplethysmography (PPG) is an optical technique that measures blood volume changes through light absorption [27], commonly deployed in smart rings or smart watches as shown in Fig. 1(f) and (g). PPG captures pulse morphology and autonomic dynamics during sleep transitions [28]. While PPG-based sleep staging methods generally achieve lower overall accuracy than scEEG-based approaches due to the indirect nature of autonomic signals [29], PPG may provide complementary information where scEEG features are ambiguous, as schematically illustrated in Fig. 1, particularly during light sleep, based on prior empirical findings [28], [30]. Furthermore, as a lightweight and low-cost sensor, PPG is accessible for augmenting scEEG-based sleep monitoring [31], [32].

This motivates investigating to what extent PPG can complement scEEG for sleep staging. Unlike EEG which directly captures cortical sleep signatures, PPG relies on indirect autonomic nervous system modulation of heart rate variability and pulse waveform characteristics [33]. These cardiovascular dynamics evolve slowly and require extended observation periods to reveal discriminative patterns, which explains why state-of-the-art (SOTA) PPG methods process full-night recordings (8 - 10 h) as input context [28], [34]. For lightweight wearable applications that require responsive feedback, short analysis windows are essential. Whether PPG can retain sufficient discriminative power under such constraints, and how to effectively combine the distinct characteristics of scEEG and PPG, remain open questions.

To address these issues, this study presents an investigation of combining scEEG and PPG for sleep staging. Leveraging existing scEEG and PPG sleep staging algorithms [30], [34], we first evaluate performance across multiple window lengths (30 s - 30 min) to study the minimal temporal context required for reliable sleep monitoring. We then investigate three fusion strategies: score-level fusion, cross-attention fusion that enables bidirectional feature-level interactions between modalities, and Mamba-enhanced fusion that incorporates temporal context modeling through selective state space models

[35]. We train and evaluate our models on the Multi-Ethnic Study of Atherosclerosis (MESA) dataset [36], a large-scale community-based sleep dataset. Furthermore, we evaluate generalizability through cross-dataset validation on the Cleveland Family Study (CFS) and the Apnea, Bariatric surgery, and CPAP (ABC) datasets [37], [38], including different populations.

The main contributions of this work are summarized as follows:

- To the best of our knowledge, this is the first study to investigate the fusion of scEEG and PPG for responsive sleep staging. We explore the feasibility of using PPG to complement scEEG for lightweight wearable sleep monitoring, addressing the limitation of scEEG in light sleep classification through multimodal fusion.
- We conduct a short-window study comparing scEEG and PPG across window lengths from 30 s to 30 min, and identify that 3-minute windows provide an effective trade-off between performance and responsiveness.
- We investigate three fusion strategies (score-level, cross-attention, and Mamba-enhanced), demonstrating that Mamba-enhanced fusion achieves the best performance (Cohen's Kappa $\kappa = 0.798$) on MESA dataset, with light sleep classification significantly improved (F1-score: 77.76% \rightarrow 85.63%, recall: 69.95% \rightarrow 82.85% for scEEG alone), and generalizes effectively to other datasets.

II. METHODOLOGY

A. Datasets

1) **MESA Dataset:** MESA is a National Heart, Lung, and Blood Institute (NHLBI)-sponsored multi-center longitudinal investigation of cardiovascular disease risk factors [39], [40]. Between 2010 and 2012, 2,237 participants were enrolled in the MESA sleep ancillary study with full overnight unattended PSG. The cohort comprises ethnically diverse participants (38% White, 28% Black, 23% Hispanic, and 11% Chinese-American) aged 54 - 93 years, representing one of the largest and most diverse community-based sleep datasets available

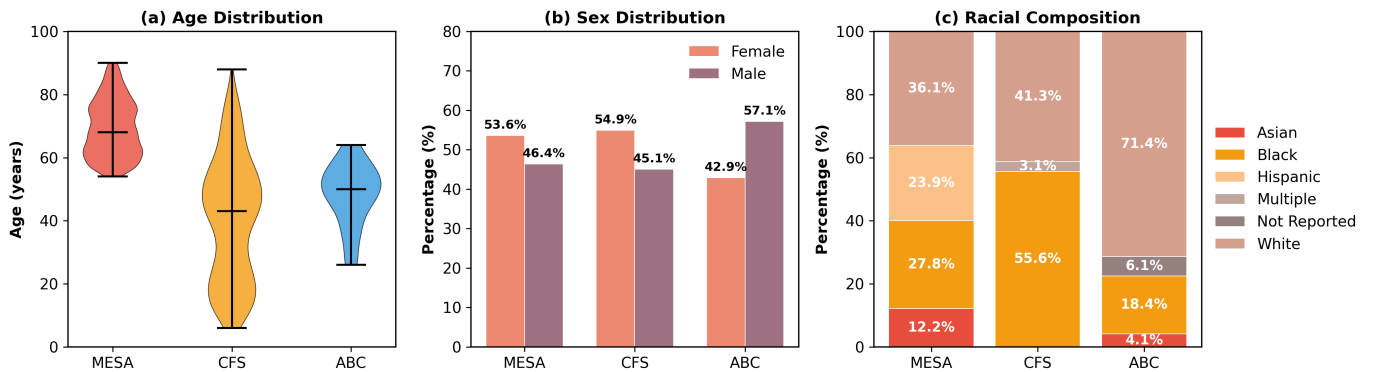


Fig. 2: Demographic characteristics of MESA, CFS and ABC datasets: (a) Age. (b) Sex distribution. (c) Racial composition highlighting MESA’s ethnic diversity, CFS’s predominantly Black and White population, and ABC’s majority White cohort.

[41]. Each PSG recording includes synchronized scEEG, PPG (from finger pulse oximetry) signals, and expert-annotated sleep stages following AASM guidelines [36]. After excluding recordings with missing or corrupted signals, 2,056 subjects are selected. Following prior work [34], we use a predefined test set of 204 subjects, with the remaining 1,852 subjects split into training and validation sets.

2) CFS Dataset: CFS is the largest family-based study of sleep apnea worldwide, comprising 2,284 individuals (46% African American) from 361 families studied over a 16-year period [37]. The study was designed to investigate genetic and non-genetic risk factors for sleep-disordered breathing. PSG recordings were collected during the fourth examination (2001-2006) at a general clinical research center, including EEG, EOG, EMG, ECG, PPG and respiratory signals with expert-scored sleep stages. For cross-dataset evaluation, we utilize 719 subjects, each contributing up to 10 hours of scEEG and PPG recordings. CFS presents distinct challenges for generalization due to differences in recording protocols, equipment, and demographic composition compared to MESA [42], including a broader age range and higher proportion of subjects with sleep-disordered breathing.

3) ABC Dataset: ABC study is a randomized clinical trial comparing bariatric surgery versus continuous positive airway pressure therapy for patients with class II obesity and severe obstructive sleep apnea (OSA) [38], [43]. The dataset includes 49 subjects who underwent baseline PSG with synchronized scEEG and PPG recordings. ABC represents a significant clinical domain shift from MESA, as participants exhibit altered sleep architecture characterized by frequent arousals, reduced deep sleep proportion, and disrupted autonomic regulation due to severe OSA. This dataset enables evaluation of model robustness under challenging pathological conditions that are common in real-world clinical populations.

Fig. 2 summarizes the demographic characteristics across all three datasets. MESA represents an older cohort (mean age 69.4 years) with substantial ethnic diversity, providing a robust foundation for model training. CFS spans a broader age range including younger participants (mean age 41.2 years) with predominantly Black (55.6%) and White (41.3%) populations. ABC comprises middle-aged adults (mean age 48.2 years) with obesity and severe OSA, predominantly White (71.4%),

representing a distinct clinical population for evaluating model robustness under pathological conditions.

B. Signal Preprocessing

1) scEEG Preprocessing: All three datasets employ mastoid-referenced EEG derivations recommended by AASM guidelines. We use a single EEG derivation from PSG as a proxy for wearable-compatible scEEG. Specifically, MESA provides C4-M1 (right central electrode referenced to left mastoid), while CFS and ABC utilize C3-M2 (left central electrode referenced to right mastoid). This setup isolates the modeling question under a single-channel constraint, while acknowledging that prospective wearable validation remains necessary (see Limitations in Section IV-D). Following the scEEG preprocessing procedure in [30], raw signals undergo bandpass filtering between 0.3 and 35 Hz and resampled to 100 Hz, yielding 3,000 samples per 30-second epoch. Continuous recordings are segmented into non-overlapping epochs aligned with expert annotations, with consecutive epochs concatenated for multi-epoch windows (1 - 30 minutes). Recording-level z-score normalization standardizes amplitude across subjects.

2) PPG Preprocessing: Following the PPG preprocessing procedure in [34], for MESA, finger photoplethysmography signals undergo 8 Hz lowpass filtering using an 8th-order Chebyshev Type II filter, followed by resampling to 34.13 Hz (1,024 samples per 30-second epoch). Values exceeding ± 3 standard deviations are clipped, and recording-level z-score normalization is applied. CFS and ABC follow identical preprocessing pipeline to ensure cross-dataset compatibility.

C. Model Architecture

1) scEEG-based model: We adopt the AttnSleep architecture [30], a well-validated model for scEEG sleep staging, which employs a Multi-Resolution Convolutional Neural Network (MRCNN) to extract hierarchical temporal features, followed by a Transformer-based temporal context encoder (TCE) with multi-head self-attention to capture long-range dependencies, as illustrated in Fig. 3(a). To handle multi-epoch windows, we extend AttnSleep by concatenating epoch-level features and feeding them into a temporal transformer (fixed 2 layers, 256 dimensions) that models cross-epoch

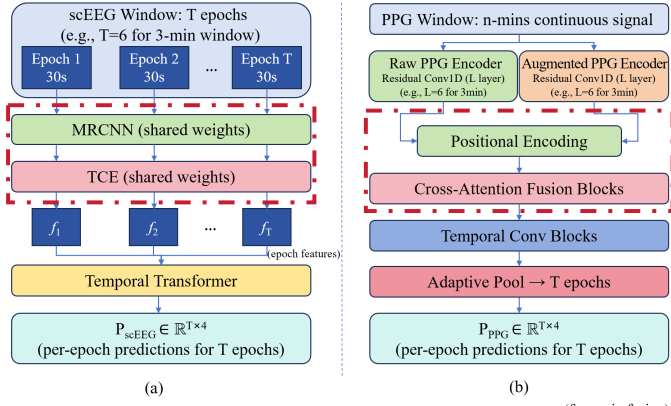


Fig. 3: Architecture of baseline models: (a) scEEG model, (b) PPG model.

dependencies. The model size remains constant across window lengths, outputting $\mathbf{P}_{\text{scEEG}} \in \mathbb{R}^{T \times 4}$, where T is the number of epochs and 4 corresponds to the sleep stage classes (Wake, Light, Deep, REM).

2) PPG-based model: We adopt a dual-stream architecture processing both raw PPG and augmented PPG through parallel residual convolutional encoders [34], as illustrated in Fig. 3(b). Cross-attention fusion blocks with bidirectional multi-head attention enable information exchange between streams, followed by temporal convolution blocks for sequence modeling. An adaptive weighting module dynamically balances the contributions of the two streams. The model outputs $\mathbf{P}_{\text{PPG}} \in \mathbb{R}^{T \times 4}$.

3) scEEG-PPG fusion: Having established separate encoders for scEEG and PPG, we now describe how to effectively combine their complementary representations. The fusion module aims to leverage the strengths of both modalities: scEEG excels at distinguishing deep sleep through delta wave patterns [44], whereas PPG provides robust features for light sleep detection through heart rate variability [45]. We study scEEG and PPG fusion strategies to improve sleep stage classification. To enable responsive sleep monitoring, both modalities are processed using aligned short windows ranging from 30 seconds to 30 minutes. In this work, we study fusion strategies, as illustrated in Fig. 4: score-level fusion, cross-attention fusion, and Mamba-enhanced fusion.

(a) Score-level fusion: As illustrated in Fig. 4(a), score-level fusion combines the probability outputs from two independently trained encoders. The scEEG-Encoder and PPG-Encoder process their respective input modalities and output probability distributions $\mathbf{P}_{\text{scEEG}}$ and \mathbf{P}_{PPG} over the four sleep stages. These distributions are combined through weighted probability fusion:

$$\mathbf{P}_{\text{score}} = \alpha \cdot \mathbf{P}_{\text{PPG}} + (1 - \alpha) \cdot \mathbf{P}_{\text{scEEG}}, \quad (1)$$

where $\alpha \in [0, 1]$ controls modality contribution. Final predictions select the class with maximum fused probability.

(b) Cross-attention fusion: Since the two modalities are time-aligned at the epoch level, cross-attention provides a principled mechanism for modality-conditioned feature reweighting: scEEG queries can select autonomic cues from PPG

features, and vice versa, as shown in Fig. 4(b). Given extracted features $\mathbf{F}_{\text{scEEG}} \in \mathbb{R}^{T \times d}$ and $\mathbf{F}_{\text{PPG}} \in \mathbb{R}^{T \times d}$ from the frozen encoders (highlighted in Fig. 3(a) and (b) in red), where $d = 256$ is the feature dimension, we apply multi-head cross-attention to allow each modality to attend to the other:

$$\mathbf{F}'_{\text{scEEG}} = \text{CrossAttn}(\mathbf{F}_{\text{scEEG}}, \mathbf{F}_{\text{PPG}}, \mathbf{F}_{\text{PPG}}) \quad (2)$$

$$\mathbf{F}'_{\text{PPG}} = \text{CrossAttn}(\mathbf{F}_{\text{PPG}}, \mathbf{F}_{\text{scEEG}}, \mathbf{F}_{\text{scEEG}}) \quad (3)$$

where $\text{CrossAttn}(Q, K, V)$ denotes multi-head cross-attention with query Q , key K , and value V . This bidirectional attention allows scEEG features to incorporate PPG’s autonomic signatures for improved light sleep identification, while PPG features leverage scEEG’s cortical information for enhanced deep sleep detection. Following standard Transformer design, each cross-attention is followed by a feed-forward network (FFN) with layer normalization and residual connections.

The attended features are processed through two cross-attention fusion blocks, then concatenated and projected to the original dimension:

$$\mathbf{F}_{\text{fused}} = \text{Linear}([\mathbf{F}'_{\text{scEEG}}; \mathbf{F}'_{\text{PPG}}]) \quad (4)$$

where $[\cdot; \cdot]$ denotes concatenation. The fused features are passed through a classification head to produce final predictions $\mathbf{P}_{\text{fused}} \in \mathbb{R}^{T \times 4}$. During training, we freeze the pre-trained scEEG/PPG encoders from Fig. 3 and only train the cross-attention blocks and classifier, reducing trainable parameters while leveraging the feature extraction capabilities learned from the single-modality models.

(c) Mamba-enhanced fusion: As depicted in Fig. 4(c), we extend the cross-attention fusion architecture by incorporating a Mamba-based temporal context module (TCM) to capture sequential dependencies across epochs. While cross-attention enables inter-modal information exchange at each epoch, it does not explicitly model the temporal evolution of sleep stages. We address this limitation by applying selective state space modeling after the cross-attention fusion.

Following Eq. (4), the fused representations $\mathbf{F}_{\text{fused}} \in \mathbb{R}^{T \times d}$ are processed through a bidirectional Mamba TCM. The Mamba block employs selective state space models (SSMs) that dynamically modulate information flow based on input content [35]. For an input sequence \mathbf{x}_t (the t -th row of $\mathbf{F}_{\text{fused}}$), the SSM computes:

$$\mathbf{h}_t = \bar{\mathbf{A}}_t \mathbf{h}_{t-1} + \bar{\mathbf{B}}_t \mathbf{x}_t \quad (5)$$

$$\mathbf{y}_t = \mathbf{C}_t \mathbf{h}_t \quad (6)$$

where \mathbf{h}_t is the hidden state, \mathbf{y}_t is the output at epoch t , and the discretized parameters $\bar{\mathbf{A}}_t$, $\bar{\mathbf{B}}_t$, and \mathbf{C}_t are input-dependent, enabling the model to selectively retain or forget information based on sleep-relevant patterns.

To capture both forward and backward temporal context, we employ a bidirectional architecture [46]. The forward Mamba block $\text{Mamba}_{\rightarrow}$ processes the sequence from $t = 1$ to T using Eqs. (5-6), while the backward block $\text{Mamba}_{\leftarrow}$ processes from $t = T$ to 1. The bidirectional outputs are then combined:

$$\mathbf{F}_{\text{temporal}} = \text{Merge}(\text{Mamba}_{\rightarrow}(\mathbf{F}_{\text{fused}}), \text{Mamba}_{\leftarrow}(\mathbf{F}_{\text{fused}})) \quad (7)$$

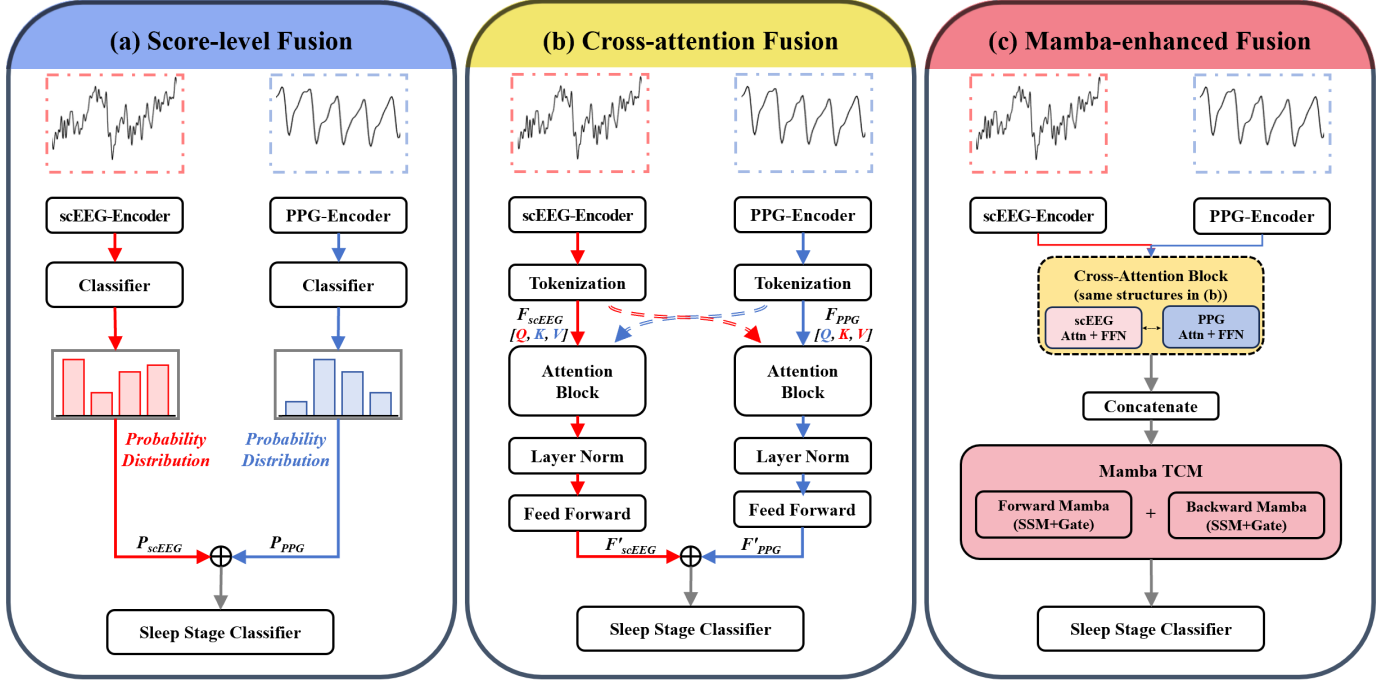


Fig. 4: Overview of three fusion strategies: (a) score-level fusion, (b) cross-attention fusion, and (c) Mamba-enhanced fusion.

where Merge combines the bidirectional outputs through linear projection. This design allows each epoch’s classification to benefit from both preceding and subsequent context, similar to how sleep experts consider adjacent epochs when scoring ambiguous transitions.

Finally, the temporal features are passed through a classification head to produce per-epoch predictions $\mathbf{P}_{\text{fused}} \in \mathbb{R}^{T \times 4}$.

D. Evaluation Metrics

1) *Performance statistics*: We evaluate model performance using accuracy (Acc) and κ . Acc measures the proportion of correctly classified epochs. κ quantifies agreement between predictions and ground truth while accounting for chance agreement: $\kappa = \frac{p_o - p_e}{1 - p_e}$, where p_o is the proportion of epochs where the model prediction matches the ground truth, and p_e is the expected proportion by random chance, providing a more robust measure for imbalanced datasets [47]. For computational efficiency analysis, we report model parameter counts (Model Size) and per-window inference (Infer.) time. For light sleep evaluation, we report recall and F1-score to assess classification performance on this challenging stage.

2) *Sleep Measures*: Beyond epoch-level classification metrics, we also compute sleep architecture measures following [48], which characterize the structural organization of sleep through clinically relevant metrics: total sleep time (TST), sleep efficiency (SE), and stage fractions including light sleep (FRLight), deep sleep (FRDeep), and REM (FRREM). These measures are defined as:

$$TST = \sum_{i=1}^n Light[i] + \sum_{i=1}^n Deep[i] + \sum_{i=1}^n REM[i] \quad (8)$$

$$SE = \frac{TST}{TST + \sum_{i=1}^n Wake[i]} \times 100 \quad (9)$$

$$FR_{Stage} = \frac{\sum_{i=1}^n Stage[i]}{TST} \times 100 \quad (10)$$

where n is the number of 30-second epochs, and $Stage[i] \in \{0, 1\}$ indicates whether epoch i belongs to the corresponding sleep stage (*Wake*, *Light*, *Deep*, or *REM*). We report mean absolute error (MAE) between predicted and reference values.

III. EXPERIMENTAL EVALUATION

A. Experimental Setup

1) *Window Length Configuration*: To study the minimal window length that achieves acceptable performance for responsive sleep staging, we evaluated six input window lengths: 30s, 1min, 3min, 5min, 10min, and 30min. For each configuration, dedicated scEEG and PPG models were trained, as illustrated in Fig. 3(a) and (b), respectively. The scEEG model extends AttnSleep [30] with a temporal transformer for cross-epoch modeling. The PPG model follows the architecture proposed in [34], with the encoder depth adjusted according to window length such that shorter windows use fewer convolutional layers. Both models were trained on the MESA dataset.

2) *Training Protocol*: Both modality-specific models were trained under a sequence-labeling objective with focal loss. The train/validation/test split followed the SleepPPG-Net protocol [28], with 204 subjects reserved for testing. All experiments were implemented in PyTorch 2.0 and executed on NVIDIA RTX 4090 GPUs. For fusion experiments, we investigated three strategies with different training requirements: (a) Score-level fusion: The fusion weight was selected via grid search over $\{0, 0.1, 0.2, \dots, 1.0\}$ on a held-out validation set, where the fused prediction is defined in Eq. (1). (b) Cross-attention fusion: The scEEG and PPG encoders (Fig. 3(a) and (b)) were frozen, and only the cross-attention layers and classifier (3.46M trainable parameters) were trained for 50 epochs

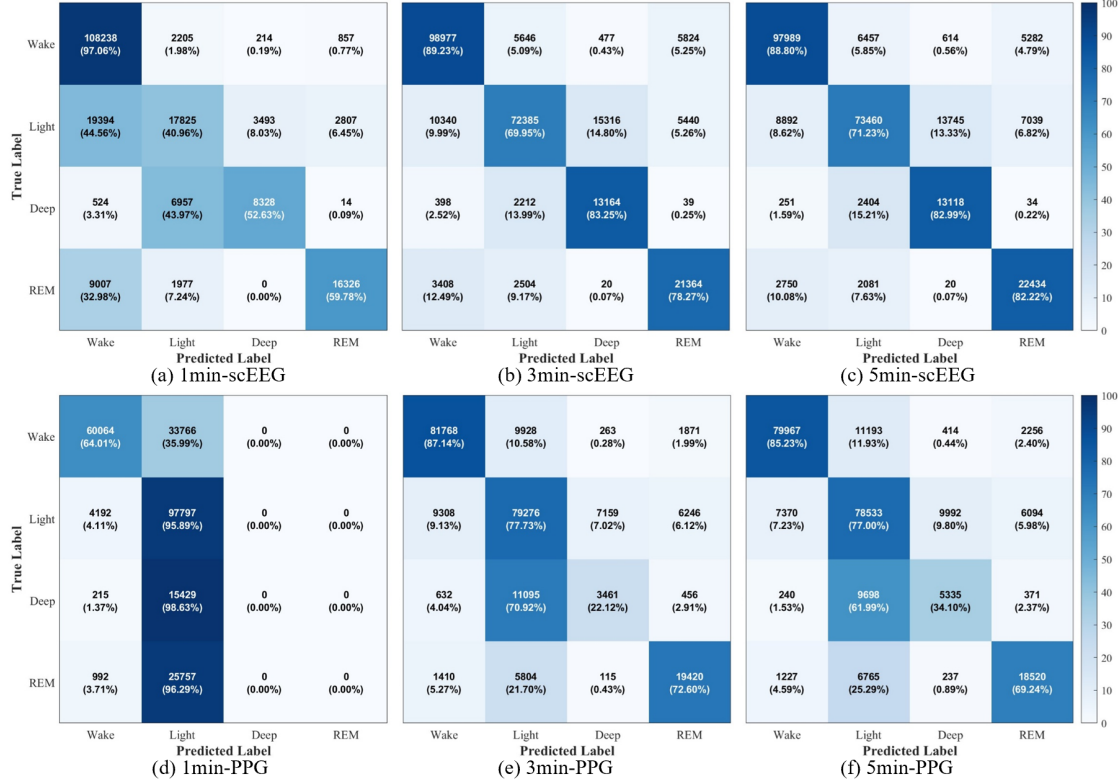


Fig. 5: Confusion matrices for sleep stage classification across different window lengths using scEEG and PPG.

with learning rate 5×10^{-4} . (c) Mamba-enhanced fusion: Building upon cross-attention fusion, the bidirectional Mamba TCM adds 1.75M trainable parameters. Training followed the same protocol as cross-attention fusion.

3) *Cross-Dataset Validation Protocol*: To assess generalization capability, we evaluated our models on CFS and ABC datasets using two paradigms: (1) direct transfer, where MESA-trained models were directly applied without adaptation, and (2) fine-tuning, where MESA-trained models were further optimized on target training data with a reduced learning rate of 1×10^{-5} and early stopping based on target validation performance. For both datasets, PPG signals were resampled to 34.13 Hz (1,024 samples per epoch) and scEEG signals were processed at 100 Hz (3,000 samples per epoch) to match MESA preprocessing. For fusion models, we adopted the fine-tuning paradigm, as the cross-attention and Mamba modules require adaptation to capture dataset-specific inter-modal relationships.

4) *Baselines*: We compare our fusion approaches against SOTA unimodal methods:

PPG-based: (1) SleepPPGNet [28], originally designed for full-night PPG recordings, processes signals through residual convolutional blocks and temporal convolution layers for 4-class sleep staging. We adapted this architecture to short-window inputs by reducing the input sequence length while preserving the core network structure. (2) Dual-stream PPG employs cross-attention fusion between raw and augmented PPG streams to extract complementary features [34].

scEEG-based: (1) AttnSleep uses multi-resolution CNNs to capture both fine-grained and coarse temporal patterns [30],

TABLE I: scEEG model performance across window lengths on MESA test set (M=204).

Window	κ	Acc	Model Size	Infer. (ms)
30 s	0.665	0.772	0.52M	3.84 ± 0.23
1 min	0.674	0.783	2.71M	3.92 ± 0.24
3 min	0.697	0.799	2.71M	3.97 ± 0.18
5 min	0.721	0.815	2.71M	3.98 ± 0.26
10 min	0.688	0.787	2.71M	3.94 ± 0.27
30 min	0.735	0.821	2.71M	3.94 ± 0.32

† Model size is constant for windows ≥ 1 min; the 30 s model uses a single-epoch setting without a temporal transformer.

TABLE II: PPG model performance across window lengths on the MESA test set (M=204).

Window	κ	Acc	Model Size	Infer.(ms)
30 s	0.460	0.647	8.28M	8.44 ± 0.56
1 min	0.538	0.701	8.29M	9.10 ± 0.68
3 min	0.643	0.772	10.26M	9.39 ± 0.39
5 min	0.633	0.758	10.26M	9.41 ± 0.55
10 min	0.656	0.777	12.23M	10.28 ± 0.59
30 min	0.696	0.804	14.20M	11.05 ± 0.60

† Encoder depth increases with window length: 4 layers (30 s), 5 layers (1 min), 6 layers (3–5 min), 7 layers (10 min), and 8 layers (30 min).

followed by transformer-based temporal context encoding with multi-head self-attention. (2) CBraMod is a foundation model pre-trained on large-scale EEG data using self-supervised learning [49]. We used the single-channel configuration and fine-tuned the model on MESA data for 4-class sleep staging using the same data preprocessing as our scEEG model.

TABLE III: Comparison of fusion models and SOTA methods under the 3-minute window on the MESA dataset.

Strategy	Method	κ	Acc	Model Size	Infer. (ms)
PPG	SleepPPGNet [28]	0.479	0.659	2.29M	8.10 \pm 0.35
	Dual-stream PPG [34]	0.643	0.772	10.26M	9.39 \pm 0.39
scEEG	AttnSleep [30]	0.697	0.799	2.71M	3.97 \pm 0.18
	CBraMod [49]	0.762	0.769	12.14M	6.18 \pm 0.79
Fusion	Score-level (ours)	0.747	0.835	12.9M	14.40 \pm 1.07
	Cross-attention (ours)	0.767	0.844	16.29M	15.69 \pm 1.27
	Mamba-enhanced (ours)	0.798	0.869	18.17M	19.98 \pm 2.37

B. Results

scEEG Model Performance. The scEEG model shows improved performance as input window length increases, with κ ranging from 0.665 (30 s) to 0.735 (30 min), as summarized in Table I. We present detailed confusion matrices for 1, 3, and 5-minute windows in Fig. 5(a-c), as these represent the practical range for responsive wearable applications while capturing the key performance transitions. As illustrated in the confusion matrices, longer windows improve overall classification consistency.

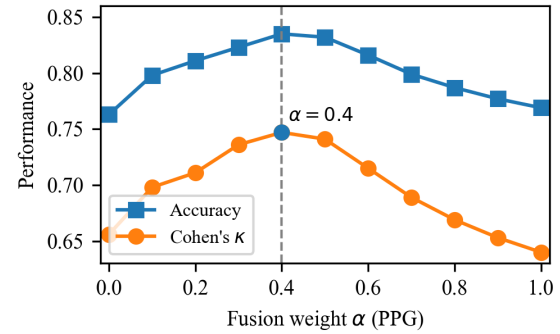
PPG Model Performance. In contrast, the PPG model shows a stronger dependence on input window length. As summarized in Table II, ultra-short windows (30 s and 1 min) result in limited discriminative capability, reflecting insufficient temporal context to capture slow-varying cardiovascular dynamics. Performance improves substantially at 3-minute windows ($\kappa = 0.643$), while longer windows yield only modest additional gains at the cost of increased model complexity. Fig. 5(d-f) presents detailed confusion matrices for 1, 3, and 5-minute windows.

Window Length Selection for Fusion. Based on these observations, we adopt a 3-minute window for subsequent scEEG-PPG fusion experiments. For scEEG, this window preserves sufficient temporal resolution for tracking sleep stage transitions while maintaining competitive classification performance. For PPG, windows shorter than 3 minutes lead to pronounced performance degradation, whereas a 3-minute window represents a reasonable duration that achieves stable and reliable classification results. Critically, a 3-minute window enables responsive sleep staging, allowing the system to provide feedback within minutes of sleep onset rather than requiring hours of data accumulation. This shared window also enables synchronized multimodal fusion with a balanced trade-off between classification performance and computational efficiency.

Fusion Method Comparison. Table III compares our fusion approaches against SOTA unimodal methods on the MESA dataset using 3-minute windows. PPG-based methods achieve κ ranging from 0.479 (SleepPPGNet) to 0.643 (Dual-stream PPG), while scEEG-based methods reach 0.697 (AttnSleep) to 0.762 (CBraMod). Although CBraMod achieves the highest unimodal κ , its model size (12.14M parameters) is over five times larger than AttnSleep (2.71M), and its accuracy (76.9%) is lower than AttnSleep (79.9%). Given the trade-off between lightweight wearable requirements and performance,

we adopted AttnSleep as the scEEG encoder for our fusion strategies.

Building upon the unimodal baselines, we investigate three fusion strategies. Score-level fusion achieves $\kappa = 0.747$, surpassing most unimodal methods. As shown in Fig. 6, the fusion weight $\alpha = 0.4$ yields the best performance, indicating that scEEG contributes more discriminative information than PPG for sleep staging. Cross-attention fusion further improves to $\kappa = 0.767$ by enabling the model to learn which features from one modality are most relevant given the other. Mamba-enhanced fusion achieves the best performance ($\kappa = 0.798$, $Acc = 86.9\%$), demonstrating that temporal context modeling across epochs provides additional discriminative power beyond feature-level fusion.

Fig. 6: Effect of fusion weight α on performance under the 3-minute window.

Sleep Architecture Estimation. Accurate sleep architecture estimation is essential for clinical sleep assessment and long-term health monitoring. As shown in Fig. 7, Mamba-enhanced fusion achieves the lowest estimation errors across most metrics, reducing TST MAE from 55.95 min (scEEG) and 30.13 min (PPG) to 13.78 min, and SE MAE from 6.87% (scEEG) and 5.19% (PPG) to 2.38%. These substantial reductions in estimation error demonstrate that multimodal fusion could provide more reliable sleep architecture metrics for home-based lightweight sleep monitoring.

Cross-dataset Evaluation. To evaluate generalization capability, we apply MESA-pretrained models to CFS and ABC datasets under two paradigms: without fine-tuning and with fine-tuning.

Table IV presents single-modality generalization results. Without fine-tuning, scEEG demonstrates strong transfer on

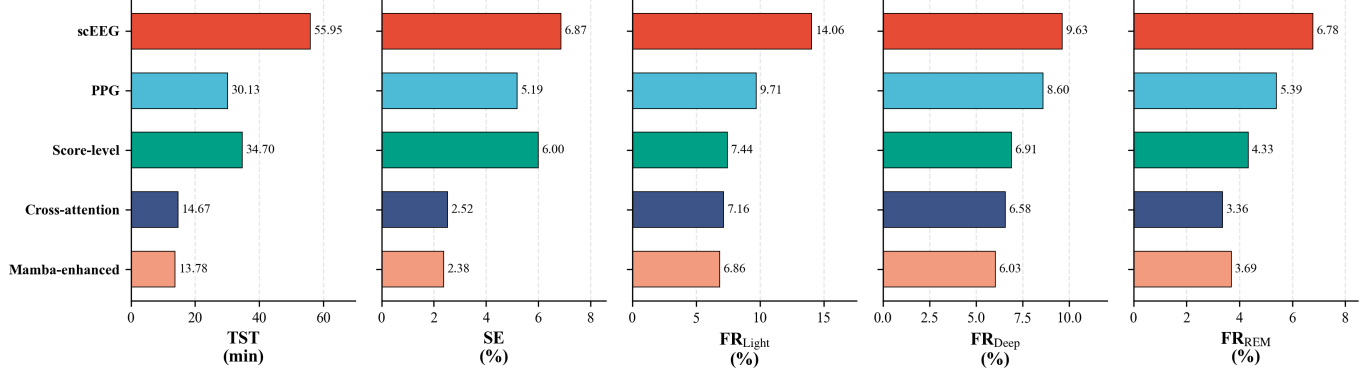


Fig. 7: Sleep architecture estimation errors (MAE) on MESA test set.

TABLE IV: Single-modality generalization performance across datasets.

Strategy	CFS		ABC	
	κ	Acc	κ	Acc
PPG (w/o fine-tuning)	0.090	0.432	0.368	0.66
scEEG (w/o fine-tuning)	0.638	0.741	0.334	0.535
PPG (fine-tuning)	0.583	0.710	0.494	0.691
scEEG (fine-tuning)	0.716	0.799	0.543	0.681

CFS ($\kappa = 0.638$) but degrades substantially on ABC ($\kappa = 0.334$), while PPG shows the opposite pattern with poor CFS transfer ($\kappa = 0.090$) but relatively better ABC transfer ($\kappa = 0.368$). This asymmetry indicates that each modality exhibits dataset-specific sensitivity, with neither consistently generalizing across all populations. After fine-tuning, both modalities improve considerably: scEEG achieves $\kappa = 0.716$ on CFS and $\kappa = 0.543$ on ABC, while PPG reaches $\kappa = 0.583$ on CFS and $\kappa = 0.494$ on ABC. These results suggest that fine-tuning remains necessary for adapting single-modality models to new populations.

TABLE V: Cross-dataset generalization performance of different fusion methods.

Dataset	Fusion Method	κ	Acc	Model Size	Infer. (ms)
CFS	Score-level	0.660	0.772	12.9M	14.62 ± 1.25
	Cross-attention	0.781	0.849	16.29M	16.05 ± 1.14
	Mamba-enhanced	0.769	0.839	18.17M	19.20 ± 1.47
ABC	Score-level	0.524	0.684	12.9M	13.38 ± 0.56
	Cross-attention	0.643	0.773	16.29M	16.13 ± 1.17
	Mamba-enhanced	0.665	0.764	18.17M	19.71 ± 1.66

Table V summarizes fusion model performance after fine-tuning. On CFS, cross-attention fusion achieves the highest performance ($\kappa = 0.781$, Acc = 84.9%), outperforming Mamba-enhanced fusion ($\kappa = 0.769$), possibly because the relatively small fine-tuning dataset favors the simpler cross-attention architecture over the Mamba-enhanced model with more trainable parameters. As shown in Fig. 8, all fusion methods substantially exceed the best single-modality result

($\kappa = 0.716$), confirming the benefit of multimodal integration.

On ABC, Mamba-enhanced fusion demonstrates the best generalization ($\kappa = 0.665$, Acc = 76.4%), followed by cross-attention fusion ($\kappa = 0.643$). The relatively lower performance compared to CFS reflects greater domain shift, as ABC has a narrower age range (26 - 64 years) and limited sample size (49 subjects), making adaptation more challenging, as shown in Fig. 2. Nevertheless, fusion methods consistently outperform single-modality methods as illustrated in Fig. 8, demonstrating that learned fusion strategies provide robust cross-dataset transfer.

IV. DISCUSSION

A. Physiological Interpretation of Modality Complementarity

A key challenge in scEEG-based sleep staging is the unreliable classification of light sleep, as evidenced by the confusion matrices in Fig. 5(b). The scEEG model achieves light sleep recall of only 69.95% and F1-score of 77.76%, substantially lower than other stages. This disparity reflects the physiological basis that light sleep exhibits subtle, low-amplitude mixed-frequency EEG activity that overlaps with wakefulness and REM patterns [50], making it difficult to distinguish from a single EEG channel.

The PPG model exhibits a complementary performance pattern. As shown in Fig. 5(e), PPG achieves higher light sleep recall (77.73%) than scEEG (69.95%). This advantage aligns with physiological principles: light sleep (N1+N2) is accompanied by a gradual shift toward parasympathetic dominance [45], producing characteristic autonomic changes that PPG can capture through pulse morphology and heart rate variability [51]. This complementary pattern provides the physiological basis for multimodal fusion.

Our fusion results confirm this complementarity. As shown in Fig. 9, the Mamba-enhanced fusion achieves light sleep recall of 82.85% and F1-score of 85.63%, substantially improving upon scEEG alone (recall: 69.95%, F1-score: 77.76%). This improvement demonstrates that PPG effectively compensates for scEEG's limitation in light sleep classification.

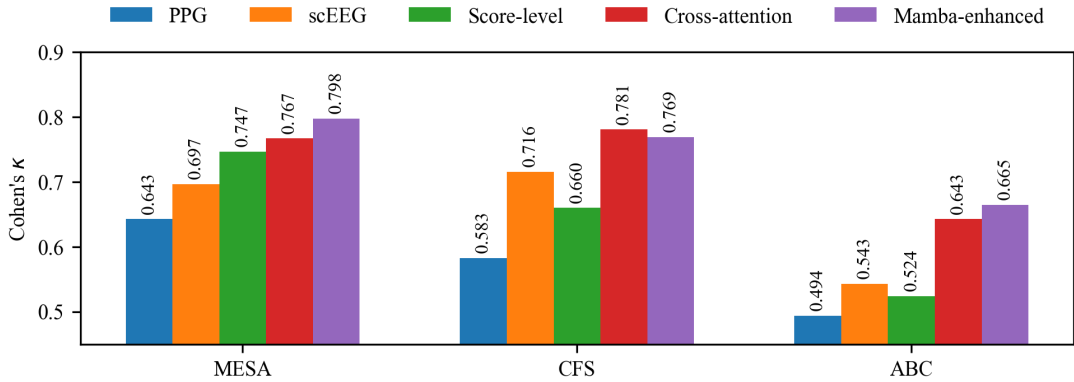


Fig. 8: Comparison of κ across single-modality and fusion-based methods on the MESA, CFS, and ABC datasets.

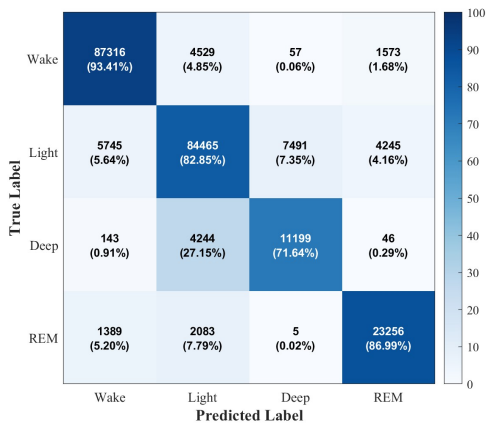


Fig. 9: Confusion matrix of the Mamba-enhanced fusion model on the MESA dataset.

B. Comparison of Fusion Strategies

The progressive improvement from score-level ($\kappa = 0.747$) to cross-attention ($\kappa = 0.767$) to Mamba-enhanced fusion ($\kappa = 0.798$) reveals two key insights. First, the improvement from score-level to cross-attention demonstrates that learned feature-level interactions capture complementary information that simple probability averaging cannot exploit. Second, the additional improvement from cross-attention to Mamba-enhanced fusion indicates that temporal context modeling provides discriminative power beyond instantaneous feature fusion. This is likely because sleep stages follow predictable transition patterns that help resolve ambiguous epochs.

C. Implications for Wearable Sleep Monitoring

Prior validation studies of wearable sleep trackers have commonly adopted acceptable thresholds of ≤ 30 min for TST and $\leq 5\%$ for SE when compared to polysomnography [52]. Our Mamba-enhanced fusion model substantially exceeds these benchmarks, achieving TST MAE of 13.78 min (54% below the 30 min threshold) and SE MAE of 2.38% (52% below the 5% threshold). These results suggest that scEEG-PPG fusion may offer a promising approach for sleep architecture

assessment in lightweight wearable devices, potentially supporting applications such as longitudinal sleep monitoring and treatment response evaluation.

D. Limitations

Several limitations should be acknowledged. First, our focus on lightweight wearable-compatible signals (scEEG and PPG) inherently limits performance compared to multi-channel EEG or multi-signal devices, representing a deliberate trade-off between clinical-grade accuracy and practical wearability. Second, we only evaluated three fusion strategies: one classical score-level fusion and two SOTA approaches (cross-attention and Mamba-enhanced). Other popular methods such as multi-task learning [53] and graph neural networks [54] should be explored in future work. Third, the scEEG signals used in this study were extracted from traditional multi-channel PSG systems (C4-M1 for MESA, C3-M2 for CFS and ABC); validation with lightweight wearable EEG devices (e.g., forehead scEEG sensors as shown in Fig. 1(d)) in naturalistic settings would better reflect real-world performance.

V. CONCLUSION

This work investigates the extent to which PPG can complement scEEG for lightweight wearable sleep staging. Our evaluation demonstrates that 3-minute windows provide an effective trade-off between classification performance and responsiveness for both modalities. Among three fusion strategies investigated, Mamba-enhanced fusion achieves the best performance ($\kappa = 0.798$, $Acc = 86.9\%$) by incorporating temporal context modeling, with notably improved light sleep classification (F1-score: 85.63% vs. 77.76%, recall: 82.85% vs. 69.95% for scEEG alone). Cross-dataset evaluation on CFS and ABC confirms that learned fusion strategies generalize effectively across populations. These findings suggest that combining scEEG and PPG as two lightweight wearable modalities is a promising approach to address scEEG's limitation in light sleep classification. This study provides evidence supporting the development of practical multimodal wearable solutions, such as smart headbands integrating both sensors, for accessible sleep health monitoring.

REFERENCES

[1] Leon Ting and Atul Malhotra. Disorders of sleep: an overview. *Primary care*, 32(2):305, 2005.

[2] Michael J Sateia. International classification of sleep disorders. *Chest*, 146(5):1387–1394, 2014.

[3] Richard B Berry, Rita Brooks, Charlene E Gamaldo, Susan M Harding, Carole Marcus, Bradley V Vaughn, et al. The aasm manual for the scoring of sleep and associated events. *Rules, Terminology and Technical Specifications, Darien, Illinois, American Academy of Sleep Medicine*, 176(2012):7, 2012.

[4] Michael H Silber. Staging sleep. *Sleep Medicine Clinics*, 7(3):487–496, 2012.

[5] Jessica Vensel Rundo and Ralph Downey III. Polysomnography. *Handbook of clinical neurology*, 160:381–392, 2019.

[6] Diana Vitazkova, Helena Kosnacova, Daniela Turonova, Erik Foltan, Martin Jagelka, Martin Berki, Michal Micjan, Ondrej Kokavec, Filip Gerhat, and Erik Vavrinsky. Transforming sleep monitoring: review of wearable and remote devices advancing home polysomnography and their role in predicting neurological disorders. *Biosensors*, 15(2):117, 2025.

[7] Wikipedia contributors. Polysomnography. <https://en.wikipedia.org/wiki/Polysomnography>. Accessed: 2025-01-01.

[8] Bing Zhai, Ignacio Perez-Pozuelo, Emma A. D. Clifton, Joao Palotti, and Yu Guan. Making sense of sleep: Multimodal sleep stage classification in a large, diverse population using movement and cardiac sensing. *Proc. ACM Interact. Mob. Wearable Ubiquitous Technol.*, 4(2), June 2020.

[9] Ignacio Perez-Pozuelo, Bing Zhai, Joao Palotti, Raghvendra Mall, Michael Aupetit, Juan M. Garcia-Gomez, Shahrad Taheri, Yu Guan, and Luis Fernandez-Luque. The future of sleep health: a data-driven revolution in sleep science and medicine. *npj Digital Medicine*, 3(1):42, 2020.

[10] Gemma L. Bate, Cameron Kirk, Rana Z. U. Rehman, Yu Guan, Alison J. Yarnall, Silvia Del Din, and Rachael A. Lawson. The role of wearable sensors to monitor physical activity and sleep patterns in older adult inpatients: A structured review. *Sensors*, 23(10), 2023.

[11] Alexander J Boe, Lori L McGee Koch, Megan K O'Brien, Nicholas Shawen, John A Rogers, Richard L Lieber, Kathryn J Reid, Phyllis C Zee, and Arun Jayaraman. Automating sleep stage classification using wireless, wearable sensors. *NPJ digital medicine*, 2(1):131, 2019.

[12] Annette Sterr, Jessica K Ebajemito, Kaare B Mikkelsen, et al. Sleep eeg derived from behind-the-ear electrodes (ceegrid) compared to standard polysomnography. *Scientific reports*, 8(1):1–12, 2018.

[13] Corinne Eicher, Cristina Gallego Vázquez, Cinzia Schmid, Patricia Sonderegger, Julia-Ramona Di Floriano, Reto Huber, Hans-Peter Landolt, Erich Seifritz, Golo Kronenberg, and Giulia Da Poian. Phase-targeted auditory stimulation to reduce sleep slow-wave activity in depressed patients at home: A feasibility study. In *ESRS SLEEP EUROPE 2024*, 2024.

[14] Yongqing Zhang, Wengpeng Cao, Lixiao Feng, Manqing Wang, Tianyu Geng, Jiliu Zhou, and Dongrui Gao. Shnn: A single-channel eeg sleep staging model based on semi-supervised learning. *Expert Systems with Applications*, 213:119288, 2023.

[15] Federico Salfi, Domenico Corigliano, Giulia Amicucci, Samantha Mombelli, Aurora D'Atri, John Axelsson, and Michele Ferrara. The potential of ensemble-based automated sleep staging on single-channel eeg signal from a wearable device. *Journal of Sleep Research*, page e70282, 2026.

[16] Waleed Nazih, Mostafa Shahin, Mohamed I Eldesouki, and Beena Ahmed. Influence of channel selection and subject's age on the performance of the single channel eeg-based automatic sleep staging algorithms. *Sensors*, 23(2):899, 2023.

[17] Shuguang Zhao, Fangfang Long, Xin Wei, Xiaoli Ni, Hui Wang, and Bokun Wei. Evaluation of a single-channel eeg-based sleep staging algorithm. *International Journal of Environmental Research and Public Health*, 19(5):2845, 2022.

[18] Greentek Sensor. Gt cap psg. <https://www.greenteksensor.com/products/eeg-caps/gt-cap-psg/>. Accessed: 2025-12-30.

[19] Neurovista Tech. Neurovista eeg sleep monitor. <https://www.neurovista.us/index.html>. Accessed: 2025-11-20.

[20] Yasir M Abdal. Eeg-based smart control system for managing multiple living room devices via eye blinking. *NTU Journal of Engineering and Technology*, 4(2), 2025.

[21] Min Wang, Cheng Chen, Hao Wu, Jianyu Zhang, Shihong Zhou, and Guoxing Wang. Will smart ring be next wave of wearables? In *2024 IEEE Biomedical Circuits and Systems Conference (BioCAS)*, pages 1–5. IEEE, 2024.

[22] Aine MacDermott, Stephen Lea, Farkhund Iqbal, Ibrahim Idowu, and Babar Shah. Forensic analysis of wearable devices: Fitbit, garmin and htp watches. In *2019 10th IFIP International Conference on New Technologies, Mobility and Security (NTMS)*, pages 1–6. IEEE, 2019.

[23] Richard B Berry, Rita Brooks, Charlene Gamaldo, Susan M Harding, Robin M Lloyd, Stuart F Quan, Matthew T Troester, and Bradley V Vaughn. Aasm scoring manual updates for 2017 (version 2.4), 2017.

[24] Jan Hedner, David P White, Atul Malhotra, Sarah Herscovici, Stephen D Pittman, Ding Zou, Ludger Grote, and Giora Pillar. Sleep staging based on autonomic signals: a multi-center validation study. *Journal of clinical sleep medicine*, 7(3):301–306, 2011.

[25] Virend K Somers et al. Sympathetic-nerve activity during sleep in normal subjects. *New England Journal of Medicine*, 328(5):303–307, 1993.

[26] John Trinder et al. Autonomic activity during human sleep as a function of time and sleep stage. *Journal of Sleep Research*, 10(4):253–264, 2001.

[27] John Allen, Dingchang Zheng, Panicos A Kyriacou, and Mohamed Elgendi. Photoplethysmography (ppg): state-of-the-art methods and applications. *Physiol. Meas.*, 42(10):100301, 2021.

[28] Kevin Kotzen, Peter H Charlton, Sharon Salabi, Lea Amar, Amir Lansberg, and Joachim A Behar. Sleepppg-net: A deep learning algorithm for robust sleep staging from continuous photoplethysmography. *IEEE Journal of Biomedical and Health Informatics*, 27(2):924–932, 2022.

[29] Ahsan Habib, Mohammad Abdul Motin, Thomas Penzel, Marimuthu Palaniswami, John Yearwood, and Chandan Karmakar. Performance of a convolutional neural network derived from ppg signal in classifying sleep stages. *IEEE Transactions on Biomedical Engineering*, 70(6):1717–1728, 2022.

[30] Emadeldeen Eldele, Zhenghua Chen, Chengyu Liu, Min Wu, Chee-Keong Kwoh, Xiaoli Li, and Cuntai Guan. An attention-based deep learning approach for sleep stage classification with single-channel eeg. *IEEE Transactions on Neural Systems and Rehabilitation Engineering*, 29:809–818, 2021.

[31] Massimiliano De Zambotti, Nicola Cellini, Aimee Goldstone, Ian M Colrain, and Fiona C Baker. Wearable sleep technology in clinical and research settings. *Medicine and science in sports and exercise*, 51(7):1538, 2019.

[32] Han Wang, Jing Wang, Zhenping Zhao, Lanjun Zhou, Hongji Xu, Jun Ji, Qianyu Shi, and Songlei Zhang. Research on night stress management and sleep staging based on ppg signal of smartwatch. In *Proceedings of the 2024 International Conference on Smart Healthcare and Wearable Intelligent Devices*, pages 36–40, 2024.

[33] Mohammad Abdul Motin, Chandan Karmakar, Marimuthu Palaniswami, Thomas Penzel, and Dinesh Kumar. Multi-stage sleep classification using photoplethysmographic sensor. *Royal Society Open Science*, 10(4):221517, 2023.

[34] Jiawei Wang, Yu Guan, Chen Chen, Ligang Zhou, Laurence T Yang, and Sai Gu. On improving ppg-based sleep staging: A pilot study. In *Companion of the 2025 ACM International Joint Conference on Pervasive and Ubiquitous Computing*, pages 1640–1644, 2025.

[35] Albert Gu and Tri Dao. Mamba: Linear-time sequence modeling with selective state spaces. In *First conference on language modeling*, 2024.

[36] Xiaoli Chen, Rui Wang, Phyllis Zee, Pamela L Lutsey, Sogol Javaheri, Carmela Alcántara, Chandra L Jackson, Michelle A Williams, and Susan Redline. Racial/ethnic differences in sleep disturbances: the multi-ethnic study of atherosclerosis (mesa). *Sleep*, 38(6):877–888, 2015.

[37] Susan Redline, Peter V Tishler, Tor D Tosteson, John Williamson, Kenneth Kump, Ilene Browner, Veronica Ferrette, and Patrick Krejci. The familial aggregation of obstructive sleep apnea. *American journal of respiratory and critical care medicine*, 151(3):682–687, 1995.

[38] Jessie P Bakker, Ali Tavakkoli, Michael Rueschman, Wei Wang, Robert Andrews, Atul Malhotra, Robert L Owens, Amit Anand, Katherine A Dudley, and Sanjay R Patel. Gastric banding surgery versus continuous positive airway pressure for obstructive sleep apnea: a randomized controlled trial. *American journal of respiratory and critical care medicine*, 197(8):1080–1083, 2018.

[39] Joon Chung, Matthew Goodman, Tianyi Huang, Meredith L Wallace, Pamela L Lutsey, Jarvis T Chen, Cecilia Castro-Diehl, Suzanne Bertisch, and Susan Redline. Multi-dimensional sleep and mortality: the multi-ethnic study of atherosclerosis. *Sleep*, 46(9):zsad048, 2023.

[40] Guo-Qiang Zhang, Licong Cui, Remo Mueller, Shiqiang Tao, Matthew Kim, Michael Rueschman, Sara Mariani, Daniel Mobley, and Susan Redline. The national sleep research resource: towards a sleep data

commons. *Journal of the American Medical Informatics Association*, 25(10):1351–1358, 2018.

[41] Ying Zhang, Matthew Kim, Michael Prerau, Daniel Mobley, Michael Rueschman, Kathryn Sparks, Meg Tully, Shaun Purcell, and Susan Redline. The national sleep research resource: making data findable, accessible, interoperable, reusable and promoting sleep science. *Sleep*, 47(7):zsae088, 2024.

[42] Huy Phan, Oliver Y Chén, Philipp Koch, Zongqing Lu, Ian McLoughlin, Alfred Mertins, and Maarten De Vos. Towards more accurate automatic sleep staging via deep transfer learning. *IEEE Transactions on Biomedical Engineering*, 68(6):1787–1798, 2020.

[43] Aharon E Sareli, Charles R Cantor, Noel N Williams, Gary Korus, Steven E Raper, Grace Pien, Sharon Hurley, Greg Maislin, and Richard J Schwab. Obstructive sleep apnea in patients undergoing bariatric surgery—a tertiary center experience. *Obesity surgery*, 21(3):316–327, 2011.

[44] Bastien Lechat, Kristy L Hansen, Yohannes Adama Melaku, Andrew Vakulin, Gorica Micić, Robert J Adams, Sarah Appleton, Danny J Eckert, Peter Catcheside, and Branko Zajamsek. A novel electroencephalogram-derived measure of disrupted delta wave activity during sleep predicts all-cause mortality risk. *Annals of the American Thoracic Society*, 19(4):649–658, 2022.

[45] Hakseung Kim, Hee Ra Jung, Jung Bin Kim, and Dong-Joo Kim. Autonomic dysfunction in sleep disorders: from neurobiological basis to potential therapeutic approaches. *Journal of clinical neurology (Seoul, Korea)*, 18(2):140, 2022.

[46] Cheol-Hui Lee, Hakseung Kim, Hyun-jee Han, Min-Kyung Jung, Byung C Yoon, and Dong-Joo Kim. Neuronet: A novel hybrid self-supervised learning framework for sleep stage classification using single-channel eeg. *arXiv preprint arXiv:2404.17585*, 2024.

[47] Jacob Cohen. A coefficient of agreement for nominal scales. *Educational and psychological measurement*, 20(1):37–46, 1960.

[48] Shirel Attia, Revital Shani Hershkovich, Alissa Tabakhov, Angeleene Ang, Arie Oksenberg, Riva Tauman, and Joachim A Behar. Sleepppgnet2: Deep learning generalization for sleep staging from photoplethysmography. *Physiological Measurement*, 46(12):125001, 2025.

[49] Jiquan Wang, Sha Zhao, Zhiling Luo, Yangxuan Zhou, Haiteng Jiang, Shijian Li, Tao Li, and Gang Pan. Cbramod: A criss-cross brain foundation model for eeg decoding. *arXiv preprint arXiv:2412.07236*, 2024.

[50] Aakash K Patel, Vamsi Reddy, Karlie R Shumway, and John F Araujo. Physiology, sleep stages. In *StatPearls [Internet]*. StatPearls Publishing, 2024.

[51] Junyung Park, Hyeyon Seok Seok, Sang-Su Kim, and Hangsik Shin. Photoplethysmogram analysis and applications: an integrative review. *Frontiers in physiology*, 12:808451, 2022.

[52] An-Marie Schyvens, Brent Peters, Nina Catharina Van Oost, Jean-Marie Aerts, Federica Masci, An Neven, Hélène Dirix, Geert Wets, Veerle Ross, and Johan Verbraecken. A performance validation of six commercial wrist-worn wearable sleep-tracking devices for sleep stage scoring compared to polysomnography. *Sleep Advances*, 6(2):zpaf021, 2025.

[53] Caihong Zhao, Jinbao Li, and Yahong Guo. Sequence signal reconstruction based multi-task deep learning for sleep staging on single-channel eeg. *Biomedical Signal Processing and Control*, 88:105615, 2024.

[54] Qi Wang, Yecai Guo, Yuhui Shen, Shuang Tong, and Hongcan Guo. Multi-layer graph attention network for sleep stage classification based on eeg. *Sensors*, 22(23):9272, 2022.